JOURNAL OF MAGNETIC RESONANCE 61, 245–253 (1985)

Zero-Field EPR of the Vanadyl Ion in Ammonium Sulfate

RICHARD BRAMLEY* AND STEVEN J. STRACH

Research School of Chemistry, Australian National University, GPO Box 4, Canberra, Australian Capital Territory 2601, Australia

Received February 28, 1984

Zero-field EPR measurements of the vanadyl ion in ammonium sulfate have allowed accurate determination of the hyperfine principal values for three physically distinct sites. This has shown that the rhombic distortions in these sites are almost constant, in contrast to results from a previous EPR analysis. Analytical expressions and polarizations are given for the zero-field resonances for the case of axial hyperfine and nuclear quadrupole terms. These, along with calculations using exact diagonalization for the rhombic case, show certain features of the spectrum to be highly sensitive to certain parameters. Line narrowing is explained by analyzing the effect of small local magnetic fields on the energy levels. © 1985 Academic Press, Inc.

The study of transition ions by swept-frequency zero-field EPR spectroscopy (ZFR) has primarily involved ions in which the zero-field splittings arise from those electron spin multiplicities which permit terms in the spin Hamiltonian involving S^2, S^4, etc., depending on the total electron spin S (*1*). Additional splittings from nuclear hyperfine interactions have been observed at zero field for Gd^{3+} (isotopically enriched) (*2*) and Mn^{2+} (*1, 3, 4*). ZFR has been observed for Cr^{3+} ($S = \frac{3}{2}$, 10% ^{53}Cr with $I = \frac{3}{2}$) in cubic MgO in which the zero-field splittings between the various F levels arise purely from the isotropic hyperfine interaction. The only previous description of ZFR of an $S = \frac{1}{2}$ transition ion in the solid state where zero-field splittings arise from hyperfine and quadrupolar interactions was that given by Erickson on Nd^{3+} ($I = \frac{7}{2}$ isotopes) in lanthanum ethyl sulfate and lanthanum chloride, where the effective spin $S = \frac{1}{2}$ (*5, 1*). In this paper we report a complete analysis of the ZFR of VO^{2+} which has electron and nuclear spin states (100% ^{51}V with $I = \frac{7}{2}$) similar to those of Nd^{3+}. Three transitions of a vanadyl species at zero magnetic field have been detected previously (*6*).

Experimental work on the oxovanadium(IV) ion VO^{2+} (commonly referred to as vanadyl) has recently been reviewed (*7*). Since this ion is frequently employed as a probe of phenomena ranging from ferroelectric phase transitions (*8*) to membrane structure and dynamics (*9*), we felt that the advantages of ZFR could usefully be studied for this ion. Greater precision for hyperfine parameters and possibly finer details of the nature of the ion environment were anticipated. We chose the vanadyl-doped ammonium sulfate system for our initial work since it has been closely examined by EPR, with g and hyperfine principal values quoted for three physically

* To whom correspondence should be addressed.

0022-2364/85 $3.00
Copyright © 1985 by Academic Press, Inc.
All rights of reproduction in any form reserved.

distinct sites in the lattice (*10*). All sites showed a slight rhombic distortion. This system represents one of the more complex vanadyl systems that have been studied by EPR.

EXPERIMENTAL

A small amount of VO^{2+} was introduced into $(NH_4)_2SO_4$ by crystallization from an aqueous solution of the ammonium salt containing 2 mol% of vanadyl sulfate. The crystals were subsequently powdered and analysis by atomic absorption spectrophotometry showed that they contained 0.44 mol% V. EPR spectroscopy (at 9.5 GHz) of the powder gave a spectrum similar to that described by Chu (*11*). We observed the zero-field resonances of polycrystalline $VO^{2+}/(NH_4)_2SO_4$ (Fig. 1a) and of its deuterated counterpart, and the resonance of a 10^{-1} *M* aqueous solution of vanadyl sulfate. The deuterated system was prepared by twice dissolving the mixture of salts in D_2O and removing the solvent by rotary evaporation. Tests on the H_2O system showed that this method of preparation did not affect the ZFR frequencies compared with the crystallization method but the concentration of VO^{2+} incorporated into the lattice was reduced.

The swept-frequency ZFR was phase detected at twice the frequency of a bidirectional square-wave magnetic field modulation. The principles of the method have been described in a recent review (*1*). In this experiment we found that the nonresonant coaxial line sample cell technique, which was satisfactory for other transition ion studies (*1, 3, 4*), gave too weak a signal. This is partly because of the relatively low concentration of vanadyl ions attainable in ammonium sulfate and partly because of the less favorable Boltzmann population factors at the lower ZFR frequencies encountered in this experiment. For this reason a resonant device was

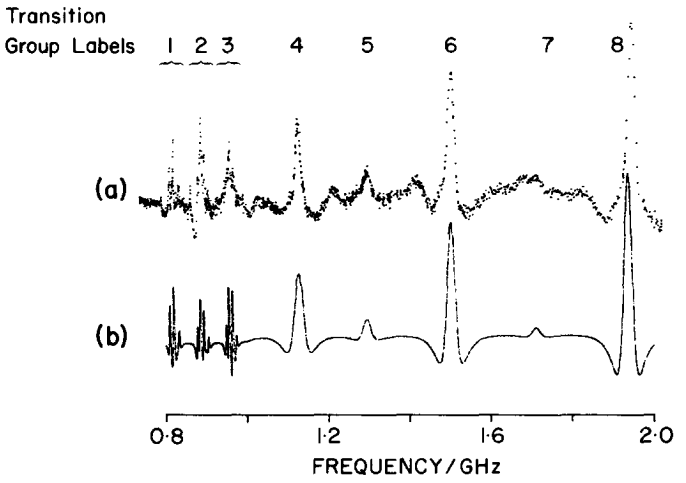

FIG. 1. (a) Experimental ZFR spectrum of $VO^{2+}/(NH_4)_2SO_4$ at 296 K. Details between 0.8 and 1.0 GHz are shown more clearly in Fig. 2. (b) Simulated spectrum using the parameter values given in Table 1. Approximations to the lineshapes were obtained using 2nd derivative Lorentzian functions (see text) of width (baseline to baseline) 5 MHz between 0.8 and 1.0 GHz and 32 MHz between 1.0 and 2.0 GHz.

used in which the frequency could be continuously varied. We used an adaptation of the recently described loop-gap resonator (*12, 13*). The shielded, single-gap resonators used were made of brass and typically had an unloaded Q of 400, as determined by a microwave network analyzer (Hewlett-Packard Model 8410A). Up to one octave range tuning was achieved by motor driving a single crystal rod of rutile down a hole drilled along the center of the gap, parallel to the resonator axis. The spectra were recorded by an automatic cycle of motor on, motor off, delay (to allow transients to decay), and record, resulting in the plots shown in Figs. 1a and 2a. Magnetic field modulation (±40 G) was produced by a Helmholtz coil pair with its axis parallel to the microwave field component. Slots cut perpendicularly to the resonator axis minimized eddy current distortion of the modulation field profile. In this parallel configuration, the gap itself serves the same purpose. A transmission arrangement was used with two coupling loops, one from the source and the other connected to the crystal detector (at the opposite end of the resonator). In the range 1 to 2 GHz where a reflection setup using a circulator had earlier been used, sensitivities were comparable with those of the transmission arrangement.

ZFR ANALYSIS

Our initial ZFR measurements on the powdered sample covered the frequency range 1 to 2 GHz and showed five resonances of width (at half maximum height) 18 MHz. These features are labeled 4 to 8 in Fig. 1a. Such a spectrum can readily be explained in terms of one vanadyl species in which there is an axial hyperfine interaction and spin Hamiltonian:

$$\mathscr{H}_s = A_{\parallel} S_z I_z + A_{\perp}(S_x I_x + S_y I_y).$$

Values $A_{\perp} = 203$, $A_{\parallel} = 541$ MHz adequately reproduced these five resonance positions. This spin Hamiltonian also predicts three more resonances between 800

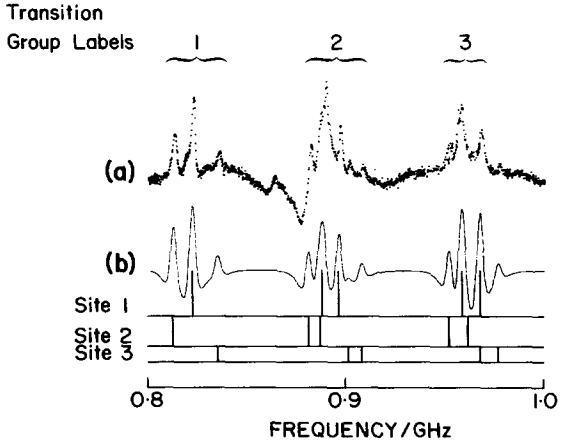

FIG. 2. (a) Details of experimental ZFR between 0.8 and 1.0 GHz. (b) Details of simulated spectrum between 0.8 and 1.0 GHz and stick diagrams relating peaks in the spectra to the three different sites. Very weak transitions (not detected) are not included in the stick diagrams.

and 1000 MHz (as well as some weak low frequency transitions between 50 and 250 MHz which have not been investigated). When the lower frequency limit of the spectrometer was extended to 750 MHz by construction of a suitable resonator, it was immediately obvious from the multitude of zero-field resonances between 800 and 1000 MHz that at least three vanadyl species were present and that their hyperfine interactions had rhombic components. The complete 800 to 2000 MHz spectrum is shown in Fig. 1a.

The observed spectrum arising from several vanadyl species is best understood by first considering the case of a single vanadyl species with an axial hyperfine interaction. In such a case analytical expressions for the resonant frequencies (*5, 1*) can be written; for completeness we include an axial nuclear quadrupole term P: $\nu_1 = 4A_\perp$, ν_2(a and b) $= \pm P + 2A_\perp + q/2$, $\nu_3 = q$, ν_4(a and b) $= \pm 3P + q/2 + r/2$, $\nu_5 = r$, ν_6(a and b) $= \pm 5P + r/2 + s/2$, $\nu_7 = s$, and $\nu_8 = 3P + 2A_\parallel + s/2$, where $q = \{(A_\parallel - 2P)^2 + 15A_\perp^2\}^{1/2}$, $r = \{4(A_\parallel - 2P)^2 + 12A_\perp^2\}^{1/2}$, and $s = \{9(A_\parallel - 2P)^2 + 7A_\perp^2\}^{1/2}$.

Transitions numbered 2, 4, 6, and 8 are induced by microwaves in which the oscillating magnetic field B_1 is perpendicular to the z axis, and transitions numbered 1, 3, 5, and 7 are induced with B_1 parallel to z. The axes refer to the VO^{2+} unit, with z being the V–O direction (*7*). Parameters can be obtained immediately by solving simultaneous equations and the $A_\parallel$ and $A_\perp$ values given above and zero value for P were obtained in this way from transitions 4 to 8. Transitions subdivided a and b in the above analytical expressions coincide when $P = 0$; splittings would only have a noticeable effect for the line widths encountered in this case for $P > 15$ MHz. For convenience we use the labels 1 to 8 in further discussion of these basic axial symmetry transitions.

When slight rhombic distortions ($A_x \neq A_y$) and sites with different ($A_x + A_y$) but similar A_z values are considered, the multiplicity of lines in the 800 to 1000 MHz region is explained. It is no longer possible to write analytical expressions for the resonant frequencies and the ZFR spectrum has to be calculated by diagonalization of the 16 × 16 matrix arising from a spin Hamiltonian:

$$\mathcal{H}_s = A_xS_xI_x + A_yS_yI_y + A_zS_zI_z + P\{I_z^2 - I(I+1)/3\}. \qquad [1]$$

Because of the very small value expected for P, and the almost axial symmetry, the principal axes of the nuclear quadrupole interaction tensor were assumed to be parallel with those of **A**, and a rhombic term was not included.

For small rhombic contributions to the hyperfine tensor, several useful features are noticeable in the spectra computed using Eq. [1]. With $A_\parallel$ and $A_\perp$ values in the region indicated previously, small rhombic distortions cause splittings of transitions 2 to 8, but no splitting of transition 1; moreover, the frequency of transition 1 does not change significantly for $|A_y - A_x| < 10$ MHz and the relation $\nu_1 = 2(A_x + A_y)$ can be used. Thus the frequencies of the three transitions in group 1 (Figs. 1a and 2a) can be used to obtain ($A_x + A_y$) for each of the three sites.

Splittings of lines 2 to 8 caused by the rhombic hyperfine component can be used to obtain $|A_y - A_x|$. For the cases under consideration, lines 4 to 8 are not detectably split (splittings are less than 2 MHz). For $|A_y - A_x| < 60$ MHz the twofold splitting of line 2 is reliably given by $1.55|A_y - A_x|$, and for the line 3 by $2|A_y - A_x|$. This

ignores some other weakly allowed transitions which are generally undetectable in the present experiments. These splittings allow the components of groups 2 and 3 (shown in Fig. 2a) to be assigned to different sites. Relative intensities lead to unambiguous assignments of transitions to the three sites as shown in Fig. 2b. Groups 1 to 3 in the spectrum allow quite accurate measurement of A_x and A_y for the three sites.

Final parameters were obtained by an iterative least squares procedure in which χ^2 was minimized, using all available resonances in the 800 to 2000 MHz range. This procedure was similar to that used for Mn(II) ZFR (*4*). The final values are given in Table 1 along with the root-mean-square deviation of calculated resonant peak frequencies from observed frequencies (RMD). The combined best fit simulated spectra for the three sites are shown in Fig. 1b with the 800 to 1000 MHz region shown in more detail in Fig. 2b. Values for A_x and A_y obtained directly from the spectra using groups 1 to 3 and the empirical relations given above are the same within the quoted error limits as those obtained from the iterative fits.

The transition intensities were computed by standard transition moment methods (*4*) and they are weighted by the transition frequency according to the Boltzmann population factor. It can be seen from Figs. 1 and 2 that the observed intensities using the loop-gap resonator agree quite well with the predicted intensities. The lineshapes were approximated by replacing each transition by a second derivative Lorentzian lineshape and summing over all possible transitions. Discrepancies in the shape of the negative wings, which originate in the bidirectional square-wave magnetic field modulation method of detecting the ZFR, are due to this approximation of using second derivative line shapes. Examination of the energy levels and allowed transitions as a function of small magnetic fields in various directions shows that the modulation field has different effects on the ZFR transitions. Figure 3b shows the effect on the energy levels of fields in the z direction. We can conclude from such calculations that it is a component of the modulation field in the z direction which is responsible for detection of ZFR transition groups 2 to 8 by a splitting of the resonances; components of the field in x or y directions are ineffective

TABLE 1

Results of Analysis of ZFR Spectra of $VO^{2+}/(NH_4)_2SO_4$ at 295.6 (±0.5) K[a]

Species:	1	2	3
Relative intensity:	17	12	4
A_x	202.9 (0.3)	201.2 (0.3)	206.2 (0.4)
A_y	207.8 (0.3)	204.8 (0.3)	211.0 (0.4)
A_z	540.9 (0.6)	541.5 (0.6)	540.3 (0.8)
P	0.0 (0.5)	−0.4 (1.0)	0.5 (0.6)
RMD	1.5	1.6	1.5
n	10	10	9

[a] Units of A, P, and RMD (root-mean-square deviation of calculated from experimental resonances) are MHz and parenthesized error values come from the minimum χ^2 fits using three times the parameter standard deviations. The number of features fitted n is also given for each site.

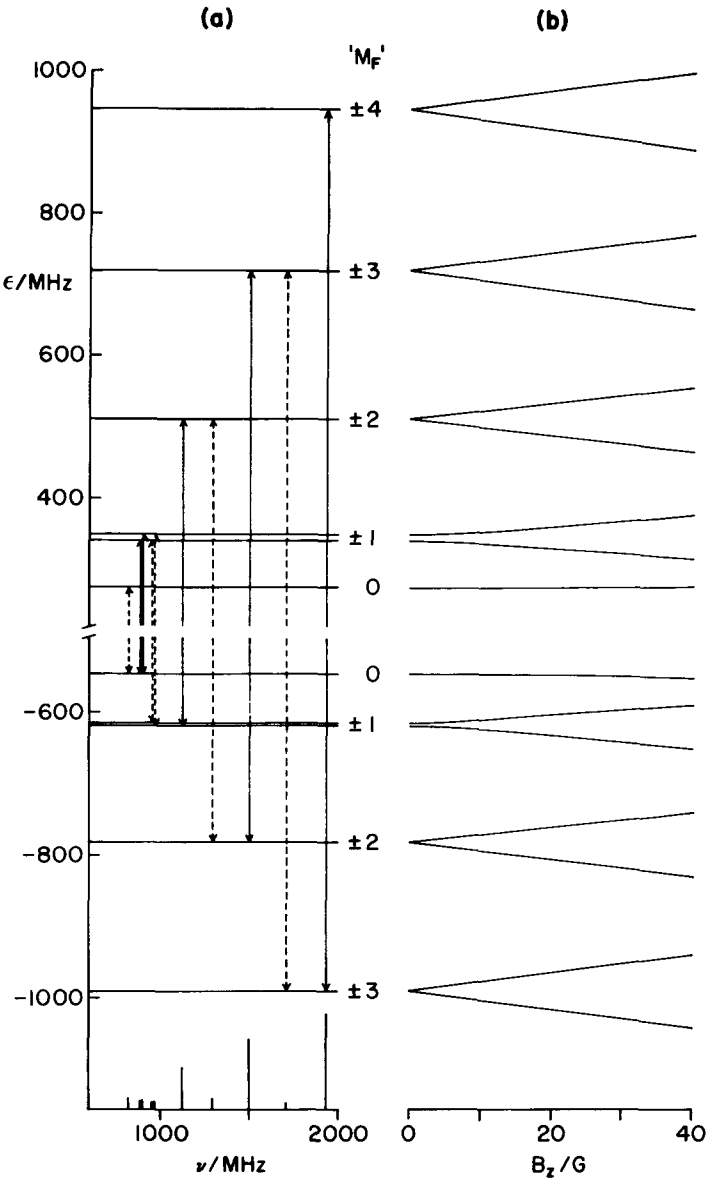

FIG. 3. (a) Zero-field energy level diagram appropriate for site 1 and the resulting ZFR transitions (excluding very weak ones) and spectrum. Transitions polarized with microwave field in the z direction are indicated by dashed lines and those with x or y polarizations are indicated by full lines. Labels "m_F" are strictly appropriate only for axial symmetry. (b) Variation of energy levels with a small magnetic field B_z along the z direction. This includes within its range the modulation fields which are effective in the powder sample in detecting the ZFR and the local fields which contribute to the linewidth of the higher frequency transitions. Fields in perpendicular directions have little effect on the levels over this range, apart from on the two "$m_F = 0$" levels on which they have a greater effect than B_z.

with the field strength used. However, for transition 1 only a component in the x and y direction shifts the transition to lower frequency and allows ZFR detection. In our experimental setup the modulation field B_m is parallel to the microwave field B_1 but the powder sample allows many combinations of components of B_m and B_1 relative to the molecular axis systems. Since we fit only peak ZFR absorption frequencies this detail of the observed lineshapes is not important in the parameter determinations.

Final values for A_z and P are somewhat less precisely determined than the other two hyperfine principal values, and P does not differ significantly from zero. Overlapping features from the three sites in groups 4 to 8 and greater linewidths of these features (which dominate the determination of A_z and P) cause this lower precision.

A fourth vanadyl site has been suggested from extra lines which appear for a few orientations of the single crystal EPR spectra (*10*). It is possible that some of the weak features in the ZFR may originate in other sites but there is insufficient information for an analysis.

DISCUSSION

ZFR has provided accurate values for the hyperfine tensor principal values for three sites of VO^{2+} in $(NH_4)_2SO_4$. For sites 1 and 2 (numbering is in decreasing order of intensity), the parameters (particularly A_x and A_y) differ very significantly from those from a single crystal EPR analysis (*10*) which gave hyperfine principal values 204.5, 220.9, 540.9 MHz for their site 1, 202.1, 217.3, 536.3 MHz for site 2 and 207.8, 211.4, 540.2 MHz for site 3 at 25°C. Our analysis shows that the rhombic distortion is much more constant for the three sites ($|A_y - A_x|$ between 3.6 and 4.9 MHz). The EPR analysis (*10*) correctly allowed for non-coincidence of **g** and **A** tensor principal axes (a problem which does not occur at zero field). Problems typical of single crystal EPR analyses such as orientational and field measurement errors as well as the approximations in using perturbation expressions for the resonant fields have probably caused the discrepancies. The 2°C difference in temperature between the two sets of measurements would make a negligible change in the parameters: ZFR transitions are the same to within experimental error at 22 and 26°C. The ZFR analysis provides a much easier and more accurate method of determining hyperfine principal values from a powder than either powder or single-crystal EPR analysis. It must be added that the **g** tensor and directional information are not available from our experiment. Principal hyperfine directions and possibly **g** tensor information (from modulation wings) would be available from single crystal intensity measurements using well polarized microwaves at zero field but we have not yet attempted such experiments apart from some on very simple systems (*1*). Comparison of the powder ZFR analysis with the powder 9 GHz EPR analysis (*11*) clearly demonstrates the power of the ZFR technique on randomly oriented samples. The powder EPR did not indicate the presence of more than one site and did not reflect the rhombic nature of the hyperfine tensor. We have found, however, that the 35 GHz powder EPR spectrum of this sample shows splitting of features indicative of two sites.

We have also examined VO^{2+} in ND_4SO_4, prepared from D_2O solutions under conditions that cause ammonium proton–deuteron exchange (*14*). The ZFR spectra

again show at least three sites, but the hyperfine parameters appear to be substantially different from those in the nondeuterated sample. The A_z values as well as A_x and A_y differ in the three sites causing transitions 4 to 8 also to split. Detailed analysis has been hampered so far by insufficient signal strength in the low-frequency transitions because the method of preparation did not allow sufficient VO^{2+} to enter the lattice. We agree with Pandey and Venkateswarlu (*10*) who deduced from the lack of proton hyperfine structure in the single-crystal EPR that water is not coordinated to the VO^{2+} ion in ammonium sulfate; such structure is readily observable in the Tutton salts (*15, 16, 17*) where the ion has five water molecules coordinated. However, there is some line narrowing of the ZFR in the deuterated salt suggesting the presence of width contributions from dipolar interactions with nearby protons in the nondeuterated case. Indications of further structure on some lines of one site in the deuterated salt suggest the possible presence of an additional nearby magnetic nucleus. We are currently looking into these effects with the object of gaining further information on the mode of incorporation of VO^{2+} into $(ND_4)_2SO_4$ and its protonated counterpart. The change in resonant frequencies on deuteration suggests that the average structure of $(ND_4)_2SO_4$ is significantly different from that of $(NH_4)_2SO_4$, at least at the level of microscopic detail revealed by ZFR, even if an EPR study (*8*) found no appreciable change on deuteration.

A notable feature of groups numbered 1 to 3 (Figs. 1a and 2a) is the much narrower line width (at half maximum height) $\Delta W_{1/2}$ which has an average value of about 2.3 MHz for these lines compared with 18 MHz for transitions 4 to 8. This leads to very precise measurements of A_x and A_y. This phenomenon has been noted for transition 1 in the similar Nd^{3+} system (*5*); in that case axial symmetry allows narrowing only for this particular line which occurs at $4A_\perp$. The ZFR of organic $-\dot{C}H-$ radicals ($S = \frac{1}{2}$, $I = \frac{1}{2}$) is subject to line narrowing (compared to EPR) of all six transitions (*18*) because of a rhombic hyperfine tensor with widely differing principal values. Such line narrowings in ZFR occur whenever the energy levels involved in a transition are subject to second-order Zeeman effects by small local magnetic fields. This occurs if the levels are nondegenerate at zero field. This is the case for transition 1 in the $S = \frac{1}{2}$, $I = \frac{7}{2}$ system in axial symmetry (levels have combined electron and nuclear spin quantum number $m_F = 0$), and for all transitions in the case of rhombic hyperfine interaction. The local field contribution to $\Delta W_{1/2}$ for groups 4 to 8 for $VO^{2+}/(NH_4)_2SO_4$ (evidently about 16 MHz) is removed for groups 1 to 3 because the energy levels are not affected to first order by small magnetic fields. Such fields arise from neighbouring magnetic nuclei by dipolar coupling: these have already been shown to be present from the deuteration experiment described above. The reason that transitions 4 to 8 are not narrowed by this process is that the energy levels are split at zero field to a much lesser extent by the rhombic component of the hyperfine tensor so their variation with applied magnetic field approaches first order at much lower fields than is the case for transitions 1 to 3. Energy level diagrams and transitions appropriate for the hyperfine principal values of site 1 are shown in Fig. 3a and the effects of small magnetic fields on the levels is shown in Fig. 3b.

It should be reiterated that the axial quadrupole interaction term P has a first-order effect on ZFR spectra unlike the higher order effect in conventional EPR spectroscopy. It may be possible to determine this interaction for VO^{2+} in a case

where overlapping lines do not occur. The most sensitive transition is that numbered 7 which for hyperfine interaction terms similar to those measured in ammonium sulfate is subject to a shift of -5.7 MHz per MHz of P. Such measurements may be useful in determining the somewhat uncertain value of Q, the nuclear quadrupole moment, of ^{51}V. The only previous reliable determinations of P, in two vanadyl-containing systems, both having $|P| < 1$ MHz, by EPR for ^{51}V have involved the use of forbidden transitions (*19*). These provided a value for Q of $-0.10 \pm 0.06b$ in reasonable accord with atomic beam measurements which gave $-0.05 \pm 0.01b$ (*20*).

The ZFR of vanadyl ions may also have applications in biological studies. Hyde *et al.* (*9*) have pointed out the usefulness of bound VO^{2+} as a spin probe to study the motions of the polar head groups of lipid molecules. ZFR may well offer a good method for evaluating the partially averaged hyperfine interactions which occur in membrane systems. Both the use of the loop-gap resonator and the fact that the transitions occur in the low microwave frequency region reduce the loss problems typical of aqueous solutions in conventional EPR spectrometers. For example, we have observed the ZFR of a 0.1 M aqueous solution of vanadyl sulfate using a loop gap resonator filled with sample as for powders. This gave a strong single resonance at 1282 (± 4) MHz of width $\Delta W_{1/2} = 85$ MHz. In this case where the hyperfine interaction is completely averaged by molecular tumbling to the isotropic value, a single line is predicted at $4A_{iso}$. (For a general I with $S = \frac{1}{2}$, resonance occurs at $(I + \frac{1}{2})A_{iso}$.) The resonant frequency is in agreement with that predicted from the literature aqueous vanadyl isotropic hyperfine interaction (*21*).

ACKNOWLEDGMENTS

We thank Miss. B. J. Stevenson and Mrs. R. Chao for the sample analysis and Dr. R. J. Robbins for providing an automatic fitting routine which was added to our $S = \frac{1}{2}$, $I = \frac{7}{2}$ ZFR/χ^2 program.

REFERENCES

1. R. BRAMLEY AND S. J. STRACH, *Chem. Rev.* **83,** 49 (1983).
2. E. R. BERNSTEIN AND G. M. DOBBS, *Phys. Rev. B* **11,** 4623 (1975).
3. R. BRAMLEY AND S. J. STRACH, *Chem. Phys. Lett.* **79,** 183 (1981).
4. S. J. STRACH AND R. BRAMLEY, *J. Magn. Reson.* **56,** 10 (1984).
5. L. E. ERICKSON, *Phys. Rev.* **143,** 295 (1966).
6. C. J. WINSCOM, personal communication.
7. R. P. KOHIN, *Magn. Reson. Rev.* **5,** 75 (1979).
8. M. FUGIMOTO, T. J. YU, AND K. FURUKAWA, *J. Phys. Chem. Solids* **39,** 345 (1978).
9. J. S. HYDE, C. A. POPP, AND S. SCHREIER, *Frontiers of Biological Energetics* **2,** 1253 (1978).
10. S. D. PANDEY AND P. VENKATESWARLU, *J. Magn. Reson.* **17,** 137 (1975).
11. K. C. CHU, *J. Magn. Reson.* **21,** 151 (1976).
12. W. N. HARDY AND L. A. WHITEHEAD, *Rev. Sci. Instrum.* **52,** 213 (1981).
13. W. FRONCISZ AND J. S. HYDE, *J. Magn. Reson.* **47,** 515 (1982).
14. M. T. EMERSON, E. GRUNWALD, M. L. KAPLAN, AND R. A. KROMHOUT, *J. Am. Chem. Soc.* **82,** 6307 (1960).
15. R. H. BORCHERTS AND C. KIKUCHI, *J. Chem. Phys.* **40,** 2270 (1964).
16. W. B. LEWIS, *Inorg. Chem.* **6,** 1737 (1967).
17. N. M. ATHERTON AND J. F. SHACKLETON, *Mol. Phys.* **39,** 1471 (1980).
18. T. COLE, T. KUSHIDA AND H. C. HELLER, *J. Chem. Phys.* **38,** 2915 (1963).
19. R. L. BELFORD, D. T. HUANG, AND H. SO, *Chem. Phys. Lett.* **14,** 592 (1972).
20. W. J. CHILDS AND L. S. GOODMAN, *Phys. Rev.* **156,** 64 (1967).
21. R. N. ROGERS AND G. E. PAKE, *J. Chem. Phys.* **33,** 1107 (1960).